Quaternary Ammonium Compounds: Bioaccumulation Potentials in Humans and Levels in Blood before and during the COVID-19 Pandemic

Guomao Zheng[1], **Thomas F. Webster**[2], **Amina Salamova**[1,*]

[1]O'Neill School of Public and Environmental Affairs, Indiana University, Bloomington 47405, United States

[2]School of Public Health, Boston University, Boston, Massachusetts 02118, United States

Abstract

Quaternary ammonium compounds (QACs) are commonly used in a variety of consumer, pharmaceutical, and medical products. In this study, bioaccumulation potentials of 18 QACs with alkyl chain lengths of C8-C18 were determined in the *in vitro–in vivo* extrapolation (IVIVE) model using the results of human hepatic metabolism and serum protein binding experiments. The slowest *in vivo* clearance rates were estimated for C12-QACs, suggesting that these compounds may preferentially build up in blood. The bioaccumulation of QACs was further confirmed by the analysis of human blood (sera) samples ($n = 222$). Fifteen out of the 18 targeted QACs were detected in blood with the ∑QAC concentrations reaching up to 68.6 ng/mL. The blood samples were collected during two distinct time periods: before the outbreak of the COVID-19 pandemic (2019; $n = 111$) and during the pandemic (2020, $n = 111$). The ∑QAC concentrations were significantly higher in samples collected during the pandemic (median 6.04 ng/mL) than in those collected before (median 3.41 ng/mL). This is the first comprehensive study on the bioaccumulation and biomonitoring of the three major QAC groups and our results provide valuable information for future epidemiological, toxicological, and risk assessment studies targeting these chemicals.

Graphical Abstract

*Corresponding author: Amina Salamova, 702 N Walnut Grove Ave., Bloomington, IN 47405 asalamov@indiana.edu.

BACs

DDACs

ATMACs
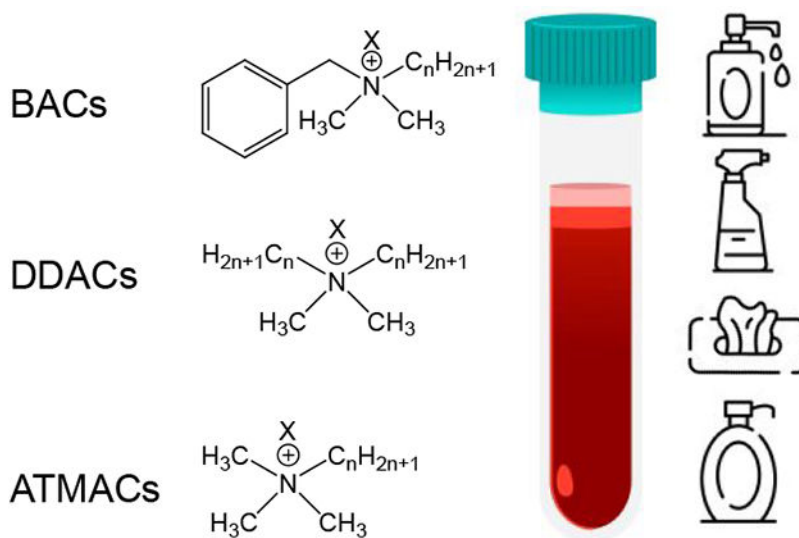
Keywords

Quaternary ammonium compounds (QACs); Disinfectants; *In vitro–in vivo* extrapolation (IVEVE); Bioaccumulation; Biomonitoring; COVID-19

INTRODUCTION

Quaternary ammonium compounds (QACs) have been extensively used as disinfectants, antimicrobials and surfactants in a variety of consumer, pharmaceutical, medical and personal care products for more than 70 years.[1] QACs are organic salts of ammonium with aryl and alkyl substitutes and the major QAC groups include benzylalkyldimethyl ammonium compounds (BACs), dialkyldimethyl ammonium compounds (DDACs), and alkyltrimethyl ammonium compounds (ATMACs) [Figure S1]. Several QACs are considered high production volume chemicals by the United States Environmental Protection Agency (U.S. EPA) with production volumes reaching up to 50 million pounds in 2015.[2]

During the coronavirus disease 2019 (COVID-19) pandemic, disinfecting of the indoor and outdoor environment has considerably increased in order to limit disease transmission, leading to the increased use of disinfecting chemicals.[1] The U.S. EPA's List N that includes disinfecting products effective against the SARS-CoV-2 has more than 200 products containing certain QACs as active ingridients.[1] In addition, more frequent hand washing with antibacterial soaps has also likely lead to the increased use of BACs that replaced triclosan banned by the United States Food and Drug Administration (U.S. FDA) in 2016.[1, 3] BACs may constitute on average about 1.8% (by weight) in soaps and multi-purpose sprays[4, 5] and DDACs and ATMACs can be intentionally or unintentionally added to surface disinfectants.[5, 6] Increased disinfection practices are likely to continue beyond the pandemic and it is anticipated that the surface disinfectant market will grow by ~10% worldwide during 2020-2027.[1] In addition, QACs are also the common ingredients in personal care and other household products.[1, 7] For example, DDACs are used in fabric softeners and ATMACs are used in cosmetics and hair conditioners.[1, 7, 8]

The large-scale manufacturing and use of these compounds have led to their widespread presence in the environment, including wastewater sludge, surface waters, sediments, and soil.[9–15] BACs (e.g., C12- and C14-BACs) and DDACs (e.g., C10-DDAC), have been found in fruits, food additives, milk and other dairy products, though their levels did not exceed the acceptable daily intake (0.1mg/kg) established by European Food Safety Authority.[16–20] We recently reported a widespread occurrence of 19 QACs, including 7 BACs, 6 DDACs and 6 ATMACs, in indoor residential dust detected at concentrations reaching up to 531 µg/g (~1% by weight).[5] A recent exposure modeling study showed that dermal contact with disinfected surfaces using QAC-containing products may result in health risks, especially for children, even if the surfaces are disinfected once a day.[4] These studies indicate that humans are widely exposed to QACs through diet, accidental dust ingestion, and dermal absorption.

There is a growing concern of the QAC toxicity. The U.S. FDA has recently requested additional safety data on certain active ingredients, including BACs, in medical and consumer antiseptic products.[21, 22] Moreover, additional scientific evidence points to the high toxicity of BACs, DDACs and ATMACs in aquatic organisms.[9] Animal studies show that skin irritation is the most frequently observed symptom of sub-chronic exposure to BACs and DDACs.[23–25] In addition, *in vitro* and *in vivo* experiments indicate that BACs and DDACs can exacerbate inflammation and disrupt mitochondrial function and cholesterol homeostasis.[26–33] Chronic exposure through a BAC-containing diet resulted in a significant decline of fertility and fecundity in both male and female mice along with increased dam mortality.[34, 35] Furthermore, maternal exposure to low levels of BACs in rodents led to neural defects in their embryos[36] and inhalation exposure to QAC-containing aerosols induced pulmonary cell damage and inflammation in rodents.[30, 31] Human epidemiological studies on the health effects of exposure to QACs are limited and mostly include occupational exposure studies linking QACs to exacerbation of asthma-related symptoms.[37–39] In a recent study, the concentrations of BACs and DDACs in human blood were associated with the increase in inflammatory cytokines, decrease in the mitochondrial function, and disruption of cholesterol homeostasis in a dose-dependent manner at levels detected in the general population[40]

The bioaccumulation potential of QACs in humans is not well understood as it has been assumed that most QACs do not bioaccumulate due to their high water-solubility [24, 25, 41] and poor intake via dermal and oral absorption (<10%).[42–46] However, there is a growing evidence showing that certain QACs can accumulate in blood and other tissues. Herron et al. (2019) has shown that dietary exposure to C12- and C16-BACs can lead to detection of these compounds in mice, including maternal blood and neonatal brain, suggesting that BACs can accumulate in tissues and even cross the blood-placental barrier.[29] A recent study reported C10-C16 BACs and C10-DDAC detected in 80% of human blood samples collected from the general US population at mean concentrations ranging from 0.01 to 1.58 ng/mL.[40] In addition, exposure models also predict that blood concentrations of C8-C18 BACs and C8-C12 DDACs in adults can range from 0.03 to 11 and 0.4 to 5.4 ng/mL, respectively.[4] The Environmental Influences on Child Health Outcomes (ECHO) program has categorized QACs as a high priority for biomonitoring in children.[47] QACs were also added to the list of priority chemicals to monitor in the general population by the Biomonitoring California program in 2021.[48]

The biological effects of chemical pollutants in organisms strongly depend on their accumulated levels in the body and are directly related to exposure levels and biotransformation processes.[49] Biotransformation rates of QACs can be measured *in vitro* and extrapolated to account for *in vivo* metabolism through clearance models.[49, 50] This approach has been used to estimate the intrinsic clearance rates for a number of environmental contaminants such as polycyclic aromatic hydrocarbons, polybrominated diphenyl ethers and organophosphate esters.[50–52] It has been previously reported that BACs were metabolized quickly in human liver microsomes through a cytochrome P450 enzyme mediated process and that their metabolic rates were dependent on the length of the alkyl chain in their structure (C10 > C12 > C14 > C16), suggesting enhanced metabolic stability of the longer chain BACs.[53] However, the human biotransformation of many other widely used QACs, including DDACs and ATMACs, has not yet been examined. Studying human metabolism of QACs would help understand the bioaccumulation potential of these compounds as well as their toxicity and provide guidance for future epidemiological and risk assessment studies.[53, 54]

Here, we conducted an *in vitro* metabolism assay using human liver microsomes and serum protein binding experiments where the *in vitro* hepatic biotransformation rates ($CL_{in\ vitro}$) and unbound fraction (f_{ub}) for 18 QACs, including 6 BACs (with alkyl chain lengths of C8-C18), 6 DDACs (C8-C18) and 6 ATMACs (C8-C18), were determined. Bioaccumulation potentials of these compounds were calculated using a hepatic clearance *in vitro–in vivo* extrapolation (IVIVE) model. We also measured these 18 QACs in human blood (sera) samples ($n = 222$) collected before and during the COVID-19 pandemic, which allowed us to evaluate the general QAC occurrence in human blood and to assess the effect of the pandemic[1, 5] on the QAC levels in blood. This is the first comprehensive study on bioaccumulation potentials and biomonitoring of the three major QAC groups and our results provide valuable information for future epidemiological, toxicological, and risk assessment studies targeting this class of compounds.

MATERIALS AND METHODS

In vitro incubations.

A reaction mixture (200 μL) of 1 mg/mL human liver microsomes (HLM, Sekisui XenoTech Inc.), 50 mM phosphate buffer (containing 3mM $MgCl_2$, pH 7.4), and 0.5 μM substrate dissolved in 0.5% (v/v) dimethyl sulfoxide was used for the *in vitro* incubation. The substrate concentration (0.5 μM) used in this study was based on the predicted blood concentration with *in vitro* bioactivity data.[4] After pre-incubation in a shaker at 37 °C for 5 min, a NADPH-generating system (NADP 6.5 mM, glucose 6-phosphate 16.5 mM, $MgCl_2$ 16.5 mM, and glucose 6-phosphate dehydrogenase 2 U/mL) was added to initiate the reaction. The incubation was performed in triplicates at 37 °C. The reaction was stopped by the addition of 200 μL of ice-cold acetonitrile after 0; 0.5; 1; 1.5; 2; 2.5; and 3 hours of incubation. A reaction with heat-deactivated microsomes was used as a negative control to assess potential background interferences and non-enzymatic changes. All incubation reactions were conducted on the same day to avoid the intra-laboratory variability. After the incubation, the mixture was ultra-sonicated with 500 μL acetonitrile for 1 hour and

centrifuged at 5000 rpm for 5 min. The supernatant was transferred into a clean vial and the residue was re-extracted with 500 μL acetonitrile twice. The combined extract was concentrated to 500 μL, filtered through a 0.2 μm nylon syringe filter and spiked with the internal standard d_7-C14-BAC.

Determination of serum protein binding affinities.

Six whole blood samples were collected from 3 males and 3 females through a venous blood draw in October 2020. The study protocol was approved by the Indiana University Institutional Review Board. The whole blood samples were centrifuged at 3000 rpm for 15 min at room temperature and the separated sera were pooled together. *In vitro* binding affinities with serum proteins were determined by the ultra-filtration method described in Beesoon and Martin (2015)[55] and Wang et al. (2020).[50] Ultra-centrifugal filters (Amicon Ultra-0.5, 10 kDa) were pre-cleaned with 25 μL of 5% Tween 80 to reduce the nonspecific binding (NSB) of QACs to the filter.[56] After centrifugation at 2000 rpm for 10 min, the residues in filters were washed out by 500 μL of 100 mM Tris buffer (pH = 7.4) twice.

One mL of serum or 100 mM Tris buffer (pH = 7.4) spiked with 0, 0.25, 0.5 and 1 μM of each target QAC (with < 1% of dimethyl sulfoxide in the incubation solution) was dispensed in 2 mL polypropylene tubes. In addition, spiked Tris buffer was used as a control to assess the NSB of QACs to the ultra-centrifugal filter. Each tube was shaken gently by hand to avoid air bubbles and then incubated at 37 °C for 1 h. After the incubation, half of the mixture (500 μL) was transferred onto a pre-cleaned ultra-centrifugal filter and centrifuged at 1500 rpm for 30 min. Hundred μL of the filtrate and 500 μL of the original sample were extracted with 1 mL acetonitrile twice. The supernatants were combined and concentrated to 500 μL using N_2. The samples were filtered through a 0.2 μm nylon syringe filter and spiked with the internal standard (d_7-C_{14}-BAC) before the instrumental analysis. All experiments were performed in triplicates.

Partitioning in blood.

Two whole blood samples (10 mL each) were collected as described above and transported to the laboratory on ice within an hour. Five mL of this sample was then used as follows: 0.3 mL was transferred into a polypropylene tube and 0.2 mL of this transferred blood was allowed to clot in a serum separation tube at room temperature and then centrifuged at 3000 rpm for 15 min to get 60 μL serum. The collected 60 μL serum and the remaining 100 μL blood were used as controls. The remaining 4.7 mL of the whole blood sample was spiked with the target QACs (0.5 μM each) and shaken gently at 37 °C. The stability of QACs during the incubation process was assessed by using 4.7 mL of 100 mM Tris buffer (pH = 7.4) spiked with the target QACs (0.5 μM each). Procedural blanks were prepared in a similar way, but without spiking the target analytes. After 0, 10, 20, 30, and 60 min, 100 μL of blood and 60 μL of serum (described above) were ultrasonicated in 1 mL of acetonitrile for 30 min twice. After centrifugation at 8000 rpm for 10 min, the supernatants were combined, transferred to a new glass tube, and concentrated to ~500 μL using N_2. Control samples of Tris buffer were diluted to 500 μL with acetonitrile. The samples were filtered through 0.2 μm nylon syringe filters and spiked with the internal standard (d_7-C_{14}-BAC).

Sample collection.

Blood (serum) samples ($n = 222$) were obtained from the Indiana University Health Biorepository. The samples were collected at Indiana University Health Methodist Hospital during February to August 2019 ($n = 111$; defined as collected before the COVID-19 pandemic) and during April to August 2020 ($n = 111$; defined as collected during the COVID-19 pandemic). Samples were stored in 2 mL polypropylene vials at −80 °C until analysis. The study protocol was approved by the Indiana University Institutional Review Board.

Sample treatment.

Each serum sample (0.5 mL, thawed at room temperature) was fortified with the surrogate standards (d_7-C12-BAC and d_9-C10-ATMAC) and ultra-sonicated in 4 mL of acetonitrile for 1 hour. The sample was then centrifuged (3000 rpm, 5 min) and the supernatant was transferred to a new tube. Each sample was re-extracted twice (total of 3 extractions), and the supernatants were combined. The sample was further concentrated to ~0.5 mL and diluted with 4 mL of 5% ammonium hydroxide in water. A clean-up method described previously was used with some modifications.[15] Briefly, the extract was loaded on an Oasis WCX cartridge (6cc, 150mg, 30μm) which was conditioned with 6 mL of methanol and 6 mL of water. After drying under vacuum, the column was then washed with 3 mL of 5% ammonium hydroxide in water (v/v) and 3 mL of methanol/water (1:9, v/v). The target analytes were eluted with 6 mL of 2% formic acid in methanol (v/v). The extract was evaporated to dryness using N_2, reconstituted in 200 μL of acetonitrile, filtered through a 0.2 μm nylon syringe filter, and spiked with the internal standard (d_7-C14-BAC).

Instrumental analysis.

The target compounds were identified and quantified on an ultra-performance liquid chromatograph coupled to a triple-quadrupole mass spectrometer (Agilent 1290 Infinity II UPLC – 6470 QQQ-MS) in the positive electrospray ionization (ESI+) mode. An Acquity UPLC BEH C_{18} column (50 mm, 2.1 mm i.d., 1.7 μm thickness, Waters) was used for the UPLC separation of the target analytes. A delay column (ZORBAX RR Eclipse Plus C_{18}, 50 mm, 4.6 mm i.d., 3.5 μm thickness, Agilent) was set up to reduce the background contamination from the instrument. The mobile phase consisted of water (A) and acetonitrile (B), both containing 0.1% formic acid. The flow rate was 0.4 mL/min. The following gradient was employed: 10% B for 0.5 min initially, ramped to 100% B at 6 min and held for 4 min, returned to 10% B at 10.5 min and equilibrated for 3.5 min after every run. The injection volume was 5 μL. The nebulizer, gas flow, gas temperature, capillary voltage, sheath gas temperature, and sheath gas flow, were set at 25 psi, 10 L/min, 300 °C, 3500 V, 350 °C, and 12 L/min, respectively. The data acquisition was conducted under a multiple reaction monitoring (MRM) mode and the optimized MRM transitions, fragmentors, and collision energies are presented in Table S1.

Quality assurance and control.

All glassware was muffled at 500°C for 6 h before use. Procedural blanks were used to monitor background contamination ($n = 12$). In addition, field blanks ($n = 6$) were

obtained using empty 2 mL polypropylene vials kept opened during blood collection to check background contamination during sampling in the hospital. Trace levels of QACs were found in procedural and field blanks but did not exceed on average 20% of the sample levels. All data were blank corrected by subtracting blank levels from the sample levels. Method detection limits (MDLs) were set at three times the standard deviation of the target analyte levels detected in the blanks. For the compounds not detected in the blanks, MDLs were based on a signal-to-noise ratio of three. Procedural and field blank levels and method detection limits for all analytes are included in Table S2. The absolute recoveries for the spiked samples (mean ± standard error) were 94 ± 1.6, 98 ± 1.6, and 91 ± 1.5% for BACs, DDACs, and ATMACs, respectively (Table S3). The mean (with standard errors) recoveries of the surrogate standards were 108 ± 4.8% and 117 ± 5.0% for d_7-C12-BAC and d_9-C10-ATMAC, respectively (Table S4).

Data analysis.

The depletion of individual QACs during the incubation with human liver microsomes followed the mono-exponential decay model (Equation 1). The *in vitro* intrinsic clearance rate ($CL_{in\ vitro}$, mL/h/mg of protein) was calculated using Equation 2:[52]

$$ln\ C_t = ln\ C_0 - k \times t \tag{1}$$

$$CL_{in\ vitro} = \frac{k}{C_{protein}} \tag{2}$$

where t is the incubation time; C_0 and C_t are the substrate concentrations at time zero and time t, respectively; k is the first-order biotransformation rate constant (h^{-1}); and $C_{protein}$ is the microsomal protein concentration (mg/mL).

The nonspecific binding (NSB, unitless) of QACs to the ultra-centrifugal filter was calculated using Equation 3:[56]

$$NSB = 1 - \frac{C_{after}}{C_{before}} \tag{3}$$

where C_{after} is the concentration of a compound in the Tris buffer after centrifugation (ng/mL); C_{before} is the concentration of that compound in the Tris buffer before centrifugation (ng/mL). These data are presented in Table S5.

The serum protein binding ratio (SPB, unitless) of a compound corrected by NSB was determined using Equation 4:[56]

$$SPB = [1 - \frac{C_{S,\ after}}{C_{S,\ before} \times (1 - NSB)}] \times 100 \tag{4}$$

where $C_{S,\ after}$ and $C_{S,\ before}$ are the concentrations of a QAC measured in serum after and before centrifugation (ng/mL), respectively.

The unbound fraction of a QAC in serum (f_{us}, unitless) and the unbound fraction of that QAC in blood (f_{ub}, unitless) were calculated using Equations 5 and 6, respectively:[56, 57]

$$f_{us} = 1 - SPB/100 \tag{5}$$

$$f_{ub} = \frac{f_{us}}{B/S} \tag{6}$$

where B/S (unitless) is the ratio of a QAC concentration in blood to that in serum after 60 min of incubation (at which point it is assumed to reach the equilibrium state) (Figure S2).

The *in vivo* hepatic clearance rate, $CL_{in\,vitro}$ (mL/h/g liver) was calculated using a scaling factor of 34 mg microsomal protein/g liver (MSP) and hepatic blood flow (Q) of 42.6 mL/h/g liver:[49]

$$CL_{in\,vivo} = \frac{Q \times f_{ub} \times CL_{in\,vitro} \times MSP/f_{um}}{Q + f_{ub} \times CL_{in\,vitro} \times MSP/f_{um}} \tag{7}$$

where the f_{um} is assumed to be 1 due to the lower protein content in the *in vitro* incubation (1 mg/mL) than that in blood (40 mg albumin/mL).[49]

Descriptive statistics and regression analyses were performed in Minitab 19 and Microsoft Excel 2016. Plots were generated in Sigma Plot 13. A Mann-Whitney test was used for the comparison of the logarithmically transformed concentrations. The non-detects were substituted with MDL/2 for all analyses. The significance level was set at $p < 0.05$.

RESULTS AND DISCUSSION

In vitro hepatic clearance rates and binding affinities.

Depletion of QACs in human liver microsomes followed the first-order kinetics and depletion curves for each QAC targeted in this study are shown in Figures S3–S5. The *in vitro* intrinsic clearance rates determined in this experiment ($CL_{in\,vitro}$) are included in Table 1. The $CL_{in\,vitro}$ values ranged from 0.042 to 1.54 mL/h/mg protein, which were up to three orders of magnitude faster than those estimated for polybrominated diphenyl ethers[51, 58] and comparable to those of polycyclic aromatic hydrocarbons[51, 59] and organophosphate esters.[50] These *in vitro* data indicate that most QACs can metabolize relatively quickly in the human liver.

Generally, $CL_{in\,vitro}$ values decreased with the increased length of the alkyl chain (Figure 1 and Table 1). A similar trend was found in a recent study that reported the human hepatic clearance rates for BACs decreased with the length of their alkyl chains (C10 > C12 > C14 > C16)[53] and in studies on biotransformation of BACs and ATMACs in aquatic organisms and bacteria.[60, 61] ATMACs were generally metabolized at slower rates than BACs and DDACs. The biotransformation rates of ATMACs ranged from 0.042 to 0.165 mL/h/mg protein, up to 10 times lower than those for BAC and DDAC homologues with the same length of the alkyl

chain. The higher metabolic stability of ATMACs can be explained by the substitution of the benzyl group in the BAC structure with a methyl group in the ATMAC structure (Figure S1), making the latter more resistant to biotransformation via oxidation (e.g., hydroxylation or epoxidation).[60, 62]

Binding affinity to blood proteins plays an important role in the pharmacokinetics and pharmacodynamics of a chemical and may affect the clearance of xenobiotics in the human liver,[49, 50, 57] where only the unbound portion of the substrate is available for metabolism.[50] The f_{ub} is the unbound fraction of QACs in blood (Table 1), which is dependent on the binding affinity of QACs to serum proteins. The f_{ub} values for the target QACs were all below 0.5 (range 0.040-0.284), indicating that only a small fraction of QACs can be transferred to and undergo metabolism in the liver. The f_{ub} generally decreased with the increasing length of the alkyl chain for the C8-C12 compounds, then increased for the C14 homologue and declined for the C16-C18 QACs. The lowest f_{ub} was found for C12-BAC (0.048) and C12-ATMAC (0.027), due to their strong binding affinities to serum proteins (Table S6 and Figure S6). The structure-dependent binding potency of these compounds could be attributed to the molecular docking mechanism[63] and was also found for per- and polyfluoroalkyl substances (PFAS) when the C8 PFAS exhibited the strongest binding affinity to serum proteins,[64–66] compared to other PFAS with shorter or longer carbon chains.

In vitro–in vivo extrapolation (IVIVE).

The *in vivo* hepatic clearance rates ($CL_{in\ vivo}$) calculated based on the *in vitro* metabolic rates and protein binding affinities (Equation 7) are given in Table 1 and Figure 1. While $CL_{in\ vivo}$ rates generally decreased with the increase in the length of the alkyl chain for all three QAC groups, the C12 homologues had the slowest *in vivo* hepatic clearance rates compared to the C14 and C16 homologues. For example, $CL_{in\ vivo}$ for C12-ATMAC was 2-4 times lower than those for C14- and C16-ATMACs. This relationship of the *in vivo* clearance rates with the length of the alkyl chain was different from that found for the *in vitro* clearance rates described in the previous section, further emphasizing the effect the binding affinities to serum proteins could have on the clearance of xenobiotics. For example, the higher binding affinity of C12-BAC to serum proteins reduces its unbound fraction in blood, which may lead to its slower clearance from the body, even though its hepatic metabolism is faster than that for the BACs with longer chain alkyl substitutes in their structure. The slower *in vivo* clearance rates of C12-QACs determined here suggest that these compounds may preferentially build up in blood. In addition, a similar $CL_{in\ vivo}$ rate was observed for C10-C16 BACs and C10-DDAC, suggesting a comparable build up potential.

Serum concentrations.

Blood samples (sera) were collected before (February - August 2019) and during the COVID-19 pandemic (April - August 2020) and population characteristics are provided in Table S7. All participants resided in Indiana, United States. The average age was 57±15 years (range 18-85 years) and the female to male ratio was 1:1. More than 80% of the participants were Caucasian, and the rest were mostly African American. Most of the

participants were non-smokers and over 80% were overweight or obese. Although the samples collected before and during the pandemic were not paired, the participants in the two groups were matched based on residence, age, gender, and smoking status. No significant relationships were found between blood QAC concentrations and participants' demographic characteristics in multivariate linear regressions.

Fifteen QACs were detected in the samples collected during the pandemic and 9 of these QACs were found in more than half of the samples (Table 2). The most frequently detected QACs in this group were C12- and C14-BACs (97 and 95% of the samples, respectively) and C14-ATMAC (94% of the samples). The total QAC concentration ($\sum$QAC, the sum of the 15 detected QACs) ranged from 0.453 to 68.6 ng/mL with a median concentration of 6.04 ng/mL. ATMACs were the most abundant QAC group found in these samples and contributed 50% to the $\sum$QAC concentrations (median $\sum$ATMAC [the sum of 4 detected ATMACs] 2.84 ng/mL), followed by the BACs (median $\sum$BAC [the sum of 6 detected BACs] 2.45 ng/mL; contribution 48%) and DDACs ($\sum$DDAC [the sum of 6 detected DDACs] 0.348 ng/mL; contribution 2%). The most abundant QAC homologues found in these samples were C14-BAC (median 1.14 ng/mL), C16-ATMAC (0.966 ng/mL) and C14-ATMAC (0.929 ng/mL).

The concentrations and detection frequencies of QACs were generally lower in the samples collected before the pandemic (Table 2). Only five QACs were detected in more than half of these samples, with C12- and C14-BACs and C12- and C14-ATMACs detected in 88-94% of the samples. These compounds were also found at the highest concentrations in this group of samples, with C12- and C14-ATMACs detected at median concentrations of 0.981 and 0.667 ng/mL, respectively, and C12- and C14-BACs found at median levels of 0.289 and 0.490 ng/mL, respectively. The contributions of the $\sum$ATMAC and $\sum$BAC concentrations to the $\sum$QAC concentrations in these samples were 66% and 34%, respectively. DDACs were detected in only a small number of the pre-COVID samples.

The $\sum$QAC concentrations in blood collected during the COVID-19 pandemic were significantly higher than those in blood collected before the pandemic ($p < 0.05$ based on a Mann-Whitney test) with the overall increase of 77% (medians 6.04 *vs.* 3.41 ng/mL, respectively; Table 2). The overall increase in the $\sum$BAC and $\sum$ATMAC concentrations was 174% and 40%, respectively ($p < 0.05$). Specifically, the levels of C12-, C14-, and C16-BACs and C14-ATMAC in samples collected during the pandemic were up to 3 times higher than those in samples collected before the pandemic (Table 2 and Figure 2). One of the possible explanations of the significant increase in BAC and ATMAC levels during the pandemic could be the increased use of household disinfecting products; however, this suggestion needs to be taken with caution as we did not collect information on the disinfectant use from the participants in this study. Our previous research shows that 72% of the households increased the disinfection frequency during the pandemic and over 80% of households regularly used QAC-containing disinfecting products. BACs contributed up to 64% to the $\sum$QAC concentrations in some of the products used in these homes (Products 1-3 from Zheng et al. 2020) and ATMACs contributed up to 82% (Products 4-7).[5] No significant change was found in the $\sum$DDAC concentrations in blood collected before and after the

pandemic, possibly due to the low detection frequencies of these QACs in both sample groups. The other possible explanation for this is that DDACs are more commonly used as antistatic and fabric softener additives than as disinfectants and thus the change of DDACs concentrations in serum is not significant as a function of the pandemic.[1] Significantly higher $\sum$QAC concentrations were found in samples collected in May, June, July, and August 2020 compared to those in samples collected during the same months of 2019 ($p <$ 0.05; Figure S7). The highest median $\sum$QAC concentration was observed in August 2020, when the pandemic was still ongoing in the United States (median 5.95 ng/mL, Figure S7).

The QACs with slower *in vivo* rates (Table 1) were detected at higher levels in serum, further suggesting a higher bioaccumulation potential for these compounds. A similar trend has been observed for organophosphate esters[50] and polybrominated diphenyl ethers[51] in previous hepatic metabolism studies. The slowest *in vivo* clearance rates (0.114-0.505 mL/h/g, respectively) were determined here for C12-C16-ATMACs, and these compounds were found at the relatively high concentrations in both sample groups. BACs that generally had faster *in vivo* clearance rates compared to ATMACs, were detected, on average, at lower concentrations than the corresponding ATMAC homologues. The levels of QACs in human serum found in this study were lower than previously reported concentrations of PFAS in serum or plasma (median 9.27-20.8 ng/mL)[69, 70] and those of synthetic phenolic antioxidants (8.52 ng/mL),[71] but higher than those of photoinitiators in serum from the United States (0.821 ng/mL).[54]

The frequent detection of QACs in human blood provides evidence of the widespread QAC exposure. Uses of QACs in various settings, including hospitals, childcare facilities, offices, and other public spaces, along with residential use, have increased significantly during the COVID-19 pandemic.[1, 5] Moreover, the increased improper use of QAC-containing products since the outbreak of the COVID-19 can exacerbate the ongoing exposure. Poison centers of the Centers for Disease Control and Prevention received more than 17,000 calls related to improper disinfectant use during January-March 2020, indicating an overall increase of 16.4% in such calls compared to 2018.[72] The elevated levels of QACs in blood collected during the pandemic found in this work could be related to the increased use of the QAC-containing disinfecting products; however, a direct connection cannot be made based on our data as the information on disinfecting practices was not collected in the current study.

Potential exposure pathways.

Our previous study has reported the first evidence of a widespread exposure to QACs in the indoor environment and suggested dust ingestion as a potential human exposure pathway to QACs.[5] Here, we compared the distribution profiles of the three QAC groups in dust reported in this previous study[5] and in blood collected during the pandemic based on the relative contribution of each QAC group to the $\sum$QAC concentrations. This comparison (Figure 3) shows that the QAC profiles in these two matrices are somewhat different (48%, 2% and 50% *vs.* 56%, 26% and 18% for BACs, DDACs and ATMACs, respectively). While both blood and dust have similar contributions of $\sum$BACs, the $\sum$ATMAC contribution in blood is much higher than that in dust, indicating that other exposure pathways may contribute to the burden of ATMACs in blood. ATMACs are more volatile based on

their lower octanol-air partitioning coefficients (log K_{OA} 8.17-11.8)[73] compared to BACs and DDACs (11.0-18.2)[73] and thus have a higher potential to evaporate from products and to partition to air, similar to other contaminants with lower log K_{OA} values such as polychlorinated biphenyls and polybrominated diphenyl ethers.[74, 75] Hence, inhalation could be another significant exposure pathway for more volatile QACs, like ATMACs. However, there are no data on the occurrence of QACs in air except one study that has reported high concentrations of C12-C16 BACs and C10-DDAC in the hospital air after spraying a QAC-containing product.[76] Our unpublished data from indoor passive polyurethane foam samplers[77] ($n = 6$) deployed in homes for 4 weeks show that indoor air ΣQAC concentrations can reach up to 4360 pg/m^3 (mean ± standard error: 3290 ± 1073 pg/m^3) with the contribution of 21%, 1% and 78% for ∑BACs, ∑DDACs and ∑ATMACs to the ∑QAC concentrations, respectively (Figure 3).[48] The high abundance of ATMACs in air suggests inhalation as a potentially important exposure pathway in the indoor environment that may lead to the build-up of ATMACs in blood. In addition to dust ingestion and inhalation, exposure to QACs via dermal absorption and mouthing-mediated ingestion of surface residues should be taken into consideration in future studies.

Strengths and limitations.

This study has several limitations. First, the molecular weight membrane cutoff of the ultracentrifugation filter used in this study was 10 kDa and did not retain some small serum proteins and peptides (< 10 kDa), which may result in underestimating the binding affinities. The clearance rates determined here for QACs only characterize the hepatic metabolism and do not account for other clearance mechanisms (e.g., biliary or renal). The extrapolation from *in vitro* to *in vivo* includes uncertainties related to the variability of scaling factors applied in the model (e.g., microsomal protein and hepatic blood flow).[49] In addition, our sample size was small and included a relatively homogenous population from a limited geographic area. The samples collected before and during the pandemic were not paired and there is a possibility of other confounding factors contributing to the difference in the QAC concentrations found between the two groups. Because we were not able to collect information on the use of disinfecting products in participants' homes, we cannot provide direct evidence showing that the increased use of disinfectants was associated with the increased levels of QACs in blood during the COVID-19 pandemic; however, this was not the main goal of this study. We were not able to collect urine samples paired with blood samples and the metabolites of QACs could not be identified. Comparison of the QAC patterns in dust, air, and blood should be considered with caution because these samples were not paired.

Nonetheless, our results provide important insights into the human hepatic biotransformation and first biomonitoring data of three QAC groups. The frequent detection of QACs in blood demonstrates a widespread human exposure in the general population. Our data highlight the importance of biomonitoring of a wide range of QACs as it reports for the first time ATMACs as the most abundant QAC group in blood. Moreover, the higher QAC concentrations in blood collected during the pandemic suggest increased exposure during this period, possibly due to the increased disinfection of the indoor and outdoor environment. Further efforts are needed to explore the relationship between the use of

QAC-containing products and the levels of QACs in human blood or of their metabolites in urine. Considering the increased use of some QACs as a result of the COVID-19 pandemic,[5] our findings warrant further exposure and epidemiological research focused on QACs.

Supplementary Material

Refer to Web version on PubMed Central for supplementary material.

Acknowledgments

REFERENCES

(1). Hora PI; Pati SG; McNamara PJ; Arnold WA, Increased use of quaternary ammonium compounds during the SARS-CoV-2 pandemic and beyond: Consideration of environmental implications. Environ. Sci. Technol. Lett 2020, 7, 622–631. [PubMed: 37566314]

(2). US EPA, Chemview. Availabe at: https://chemview.epa.gov/chemview (accessed August 2020).

(3). McNamara PJ; Levy SB, Triclosan: an instructive tale. Antimicrob. Agents Chemother 2016, 60, 7015–7016. [PubMed: 27736758]

(4). Li D; Sangion A; Li L, Evaluating consumer exposure to disinfecting chemicals against coronavirus disease 2019 (COVID-19) and associated health risks. Environ. Int 2020, 106108.

(5). Zheng G; Filippelli GM; Salamova A, Increased indoor exposure to commonly used disinfectants during the COVID-19 pandemic. Environ. Sci. Technol. Lett 2020, 7, 760–765. [PubMed: 37566290]

(6). Buffet-Bataillon S; Tattevin P; Bonnaure-Mallet M; Jolivet-Gougeon A, Emergence of resistance to antibacterial agents: the role of quaternary ammonium compounds—a critical review. Int. J. Antimicrob. Agents 2012, 39, 381–389. [PubMed: 22421329]

(7). Rahn OVE, W. P, Quaternary ammonium compounds. Annu. Rev. Microbiol 1947, 1, 173–192.

(8). Becker LC; Bergfeld WF; Belsito DV; Hill RA; Klaassen CD; Liebler D; Marks JG; Shank RC; Slaga TJ; Snyder PW; Andersen FA, Safety assessment of trimoniums as used in cosmetics. Int. J. Toxicol 2012, 31, 296S–341S. [PubMed: 23283705]

(9). Zhang C; Cui F; Zeng GM; Jiang M; Yang ZZ; Yu ZG; Zhu MY; Shen LQ, Quaternary ammonium compounds (QACs): A review on occurrence, fate and toxicity in the environment. Sci. Total Environ 2015, 518, 352–362. [PubMed: 25770948]

(10). Mulder I; Siemens J; Sentek V; Amelung W; Smalla K; Jechalke S, Quaternary ammonium compounds in soil: Implications for antibiotic resistance development. Rev. Environ. Sci. Biotechnol 2017, 17, 159–185.

(11). Jardak K; Drogui P; Daghrir R, Surfactants in aquatic and terrestrial environment: Occurrence, behavior, and treatment processes. Environ. Sci. Pollut. Res 2016, 23, 3195–3216.

(12). Harrison KR; Kappell AD; McNamara PJ, Benzalkonium chloride alters phenotypic and genotypic antibiotic resistance profiles in a source water used for drinking water treatment. Environ. Pollut 2020, 257, 113472. [PubMed: 31767233]

(13). Li X; Doherty AC; Brownawell B; Lara-Martin PA, Distribution and diagenetic fate of synthetic surfactants and their metabolites in sewage-impacted estuarine sediments. Environ. Pollut 2018, 242, 209–218. [PubMed: 29980039]

(14). Li X; Brownawell BJ, Quaternary ammonium compounds in urban estuarine sediment environments - A class of contaminants in need of increased attention? Environ. Sci. Technol 2010, 44, 7561–7568. [PubMed: 20804121]

(15). Pati SG; Arnold WA, Comprehensive screening of quaternary ammonium surfactants and ionic liquids in wastewater effluents and lake sediments. Environ. Sci. Process Impacts 2020, 22, 430–441. [PubMed: 32003378]

(16). Xian Y; Dong H; Wu Y; Guo X; Hou X; Wang B, QuEChERS-based purification method coupled to ultrahigh performance liquid chromatography-tandem mass spectrometry (UPLC-MS/MS) to determine six quaternary ammonium compounds (QACs) in dairy products. Food Chem. 2016, 212, 96–103. [PubMed: 27374511]

(17). Yu L; Malik S; Duncan TV; Jablonski JE, High throughput quantification of quaternary ammonium cations in food simulants by flow-injection mass spectrometry. J. AOAC Int 2018, 101, 1873–1880. [PubMed: 29852893]

(18). Slimani K; Feret A; Pirotais Y; Maris P; Abjean JP; Hurtaud-Pessel D, Liquid chromatography-tandem mass spectrometry multiresidue method for the analysis of quaternary ammonium compounds in cheese and milk products: Development and validation using the total error approach. J. Chromatogr. A 2017, 1517, 86–96. [PubMed: 28851528]

(19). BfR opinion No 032/2012, Health assessment of benzalkonium chloride residues in food. 2012

(20). BfR opinion No 027/2012, Health assessment of didecyldimethylammonium chloride (DDAC) residues in food 2012.

(21). US FDA., Safety and effectiveness of health care antiseptics; topical antimicrobial drug products for over-the-counter human use; Proposed amendment of the tentative final monograph; Reopening of administrative record. Federal Register 21 CFR Part. 2015, 310, 25165–25205.

(22). US FDA., Safety and effectiveness of consumer antiseptics; Topical antimicrobial drug products for over-the-counter human use; Proposed amendment of the tentative final monograph; Reopening of administrative record. Federal Register 21 CFR Part. 2016, 310, 42911–42937.

(23). Anderson SE; Shane H; Long C; Lukomska E; Meade BJ; Marshall NB, Evaluation of the irritancy and hypersensitivity potential following topical application of didecyldimethylammonium chloride. J. Immunotoxicol 2016, 13, 557–566. [PubMed: 27216637]

(24). US EPA, Alkyl Dimethyl benzyl ammonium chloride (ADBAC) final work plan, 2017, Available at: https://www.regulations.gov/contentStreamer?documentId=EPA-HQ-OPP-2015-0737-0004&contentTvpe=pdf. (accessed August 2020).

(25). US EPA, Didecyl dimethyl ammonium chloride (DDAC) final work plan, 2017, Available at: https://www.regulations.gov/contentStreamer?documentId=EPA-HQ-OPP-2015-0740-0004&contentType=pdf. (accessed August 2020).

(26). Datta S; He G; Tomilov A; Sahdeo S; Denison MS; Cortopassi G, In vitro evaluation of mitochondrial function and estrogen signaling in cell lines exposed to the antiseptic cetylpyridinium chloride. Environ. Health Perspect 2017, 125, 087015. [PubMed: 28885978]

(27). Herron J; Reese RC; Tallman KA; Narayanaswamy R; Porter NA; Xu L, Identification of environmental quaternary ammonium compounds as direct inhibitors of cholesterol biosynthesis. Toxicol. Sci 2016, 151, 261–270. [PubMed: 26919959]

(28). Herron J; Hines KM; Xu L, Assessment of altered cholesterol homeostasis by xenobiotics using ultra-high performance liquid chromatography-tandem mass spectrometry. Curr. Protoc. Toxicol 2018, 78, 65–65.

(29). Herron JM; Hines KM; Tomita H; Seguin RP; Cui JY; Xu L, Multi-omics investigation reveals benzalkonium chloride disinfectants alter sterol and lipid homeostasis in the mouse neonatal brain. Toxicol. Sci 2019, 171, 32–45. [PubMed: 31199489]

(30). Larsen ST; Verder H; Nielsen GD, Airway effects of inhaled quaternary ammonium compounds in mice. Basic Clin. Pharmacol. Toxicol 2012, 110, 537–543. [PubMed: 22188809]

(31). Kwon D; Kwon J-T; Lim Y-M; Shim I; Kim E; Lee D-H; Yoon B-I; Kim P; Kim H-M, Inhalation toxicity of benzalkonium chloride and triethylene glycol mixture in rats. Toxicol. Appl. Pharmacol 2019, 378, 114609. [PubMed: 31173787]

(32). Inácio ÂS; Costa GN; Domingues NS; Santos MS; Moreno AJM; Vaz WLC; Vieira OV, Mitochondrial dysfunction is the focus of quaternary ammonium surfactant toxicity to mammalian epithelial cells. Antimicrob. Agents Chemother 2013, 57, 2631–2639. [PubMed: 23529737]

(33). Xu L; Porter NA, Free radical oxidation of cholesterol and its precursors: Implications in cholesterol biosynthesis disorders. Free Radical Res 2015, 49, 835–849. [PubMed: 25381800]

(34). Melin VE; Melin TE; Dessify BJ; Nguyen CT; Shea CS; Hrubec TC, Quaternary ammonium disinfectants cause subfertility in mice by targeting both male and female reproductive processes. Reprod. Toxicol 2016, 59, 159–166. [PubMed: 26582257]

(35). Melin VE; Potineni H; Hunt P; Griswold J; Siems B; Werre SR; Hrubec TC, Exposure to common quaternary ammonium disinfectants decreases fertility in mice. Reprod. Toxicol 2014, 50, 163–170. [PubMed: 25483128]

(36). Hrubec TC; Melin VE; Shea CS; Ferguson EE; Garofola C; Repine CM; Chapman TW; Patel HR; Razvi RM; Sugrue JE; Potineni H; Magnin-Bissel G; Hunt PA, Ambient and dosed exposure to quaternary ammonium disinfectants causes neural tube defects in rodents. Birth Defects Res. 2017, 109, 1166–1178. [PubMed: 28618200]

(37). LaKind JS; Goodman M, Methodological evaluation of human research on asthmagenicity and occupational cleaning: a case study of quaternary ammonium compounds ("quats"). Allergy Asthma Clin. Immunol 2019, 15, 69. [PubMed: 31832071]

(38). Dumas O; Varraso R; Boggs KM; Quinot C; Zock JP; Henneberger PK; Speizer FE; Le Moual N; Camargo CA Jr., Association of occupational exposure to disinfectants with incidence of chronic obstructive pulmonary disease among US female nurses. JAMA network open 2019, 2, e1913563. [PubMed: 31626315]

(39). Walters GI; Burge PS; Moore VC; Robertson AS, Cleaning agent occupational asthma in the West Midlands, UK: 2000–16. Occup. Med 2018, 68, 530–536.

(40). Hrubec TC; Seguin RP; Xu L; Cortopassi GA; Datta S; Hanlon AL; Lozano AJ; McDonald VA; Healy CA; Anderson TC; Musse NA; Williams RT, Altered toxicological endpoints in humans from common quaternary ammonium compound disinfectant exposure. Toxicol. Rep 2021, 8, 646–656. [PubMed: 33868951]

(41). Ying G-G, Fate, behavior and effects of surfactants and their degradation products in the environment. Environ. Int 2006, 32, 417–431. [PubMed: 16125241]

(42). Luz A; DeLeo P; Pechacek N; Freemantle M, Human health hazard assessment of quaternary ammonium compounds: Didecyl dimethyl ammonium chloride and alkyl (C12–C16) dimethyl benzyl ammonium chloride. Regul. Toxicol. Pharm 2020, 116, 104717.

(43). ECHA, 2015a. Assessment report – Didecyldimethylammonium chloride product-type 8 (Wood Preservative). European Chemicals Agency. .

(44). ECHA, 2015b. Assessment report – Alkyl (C12-16) dimethylbenzyl ammonium chloride product-type 8 (Wood Preservative). European Chemicals Agency. .

(45). EPA, 2006a. Reregistration ligibility Decision (RED) for aliphatic alkyl quaternaries. EPA739-R-06-008. U.S. Environmental Protection Agency.

(46). EPA, 2006b. Reregistration Eligibility Decision (RED) for alkyl dimethyl benzyl ammonium chloride (ADBAC). EPA739-R-06-009. U.S. Environmental Protection Agency.

(47). Pellizzari ED; Woodruff TJ; Boyles RR; Kannan K; Beamer PI; Buckley JP; Wang A; Zhu Y; Bennett DH, Identifying and prioritizing chemicals with uncertain burden of exposure: Opportunities for biomonitoring and health-related research. Environ. Health Perspect 2019, 127, 126001. [PubMed: 31850800]

(48). Meeting of the scientific guidance panel for Biomonitoring California, 2021, Potential priority chemicals: Quaternary ammonium compounds, Available at: https://biomonitoring.ca.gov/sites/default/files/downloads/PotenPriorQACs030821.pdf (accessed on May 1 2021).

(49). Lipscomb JC; Poet TS, In vitro measurements of metabolism for application in pharmacokinetic modeling. Pharmacol. Ther 2008, 118, 82–103. [PubMed: 18374419]

(50). Wang X; Liu Q; Zhong W; Yang L; Yang J; Covaci A; Zhu L, Estimating renal and hepatic clearance rates of organophosphate esters in humans: Impacts of intrinsic metabolism and binding affinity with plasma proteins. Environ. Int 2020, 134, 105321. [PubMed: 31783242]

(51). Gao S; Wan Y; Zheng G; Luo K; Kannan K; Giesy JP; Lam MHW; Hu J, Organobromine compound profiling in human adipose: Assessment of sources of bromophenol. Environ. Pollut 2015, 204, 81–89. [PubMed: 25935608]

(52). Zheng G; Wan Y; Hu J, Intrinsic clearance of xenobiotic chemicals by liver microsomes: Assessment of trophic magnification potentials. Environ. Sci. Technol 2016, 50, 6343–6353. [PubMed: 27152959]

(53). Seguin RP; Herron JM; Lopez VA; Dempsey JL; Xu L, Metabolism of benzalkonium chlorides by human hepatic cytochromes P450. Chem. Res. Toxicol 2019, 32, 2466–2478. [PubMed: 31730751]

(54). Liu R; Mabury SA, First detection of photoinitiators and metabolites in human sera from United States donors. Environ. Sci. Technol 2018, 52, 10089–10096. [PubMed: 30063130]

(55). Beesoon S; Martin JW, Isomer-specific binding affinity of perfluorooctanesulfonate (PFOS) and perfluorooctanoate (PFOA) to serum proteins. Environ. Sci. Technol 2015, 49, 5722–5731. [PubMed: 25826685]

(56). Lee K-J; Mower R; Hollenbeck T; Castelo J; Johnson N; Gordon P; Sinko PJ; Holme K; Lee Y-H, Modulation of nonspecific binding in ultrafiltration protein binding studies. Pharm. Res 2003, 20, 1015–1021. [PubMed: 12880287]

(57). Leung L; Yang X; Strelevitz TJ; Montgomery J; Brown MF; Zientek MA; Banfield C; Gilbert AM; Thorarensen A; Dowty ME, Clearance prediction of targeted covalent inhibitors by in vitro-in vivo extrapolation of hepatic and extrahepatic clearance mechanisms. Drug Metab. Disposition 2017, 45, 1.

(58). Lupton SJ; McGarrigle BP; Olson JR; Wood TD; Aga DS, Human liver microsome-mediated metabolism of brominated diphenyl ethers 47, 99, and 153 and identification of their major metabolites. Chem. Res. Toxicol 2009, 22, 1802–1809. [PubMed: 19835403]

(59). Smith JN; Mehinagic D; Nag S; Crowell SR; Corley RA, In vitro metabolism of benzo[a]pyrene-7,8-dihydrodiol and dibenzo[def,p]chrysene-11,12 diol in rodent and human hepatic microsomes. Toxicol. Lett 2017, 269, 23–32. [PubMed: 28119020]

(60). Garcia MT; Ribosa I; Guindulain T; Sánchez-Leal J; Vives-Rego J, Fate and effect of monoalkyl quaternary ammonium surfactants in the aquatic environment. Environ. Pollut 2001, 111, 169–175. [PubMed: 11202711]

(61). Nishiyama N; Toshima Y; Ikeda Y, Biodegradation of alkyltrimethylammonium salts in activated sludge. Chemosphere 1995, 30, 593–603. [PubMed: 7889347]

(62). Testa B; Pedretti A; Vistoli G, Reactions and enzymes in the metabolism of drugs and other xenobiotics. Drug Discov. Today 2012, 17, 549–560. [PubMed: 22305937]

(63). Ren X-M; Qin W-P; Cao L-Y; Zhang J; Yang Y; Wan B; Guo L-H, Binding interactions of perfluoroalkyl substances with thyroid hormone transport proteins and potential toxicological implications. Toxicology 2016, 366–367, 32-42.

(64). McManaman JL, Lipid transport in the lactating mammary gland. J. Mammary Gland Biol. Neoplasia 2014, 19, 35–42. [PubMed: 24567110]

(65). MacManus-Spencer LA; Tse ML; Hebert PC; Bischel HN; Luthy RG, Binding of perfluorocarboxylates to serum albumin: A comparison of analytical methods. Anal. Chem 2010, 82, 974–981. [PubMed: 20039637]

(66). Zhang LY; Ren XM; Guo LH, Structure-based investigation on the interaction of perfluorinated compounds with human liver fatty acid binding protein. Environ. Sci. Technol 2013, 47, 11293–11301. [PubMed: 24006842]

(67). Ruan T; Song S; Wang T; Liu R; Lin Y; Jiang G, Identification and composition of emerging quaternary ammonium compounds in municipal sewage sludge in China. Environ. Sci. Technol 2014, 48, 4289–4297. [PubMed: 24654682]

(68). Kierkegaard A; Sundbom M; Yuan B; Armitage JM; Arnot JA; Droge STJ; McLachlan MS, Bioconcentration of several series of cationic surfactants in rainbow trout. Environ. Sci. Technol 2021, 55, 8888–8897. [PubMed: 34133133]

(69). Kotlarz N; McCord J; Collier D; Lea CS; Strynar M; Lindstrom Andrew B; Wilkie Adrien A; Islam Jessica Y; Matney K; Tarte P; Polera ME; Burdette K; DeWitt J; May K; Smart Robert C; Knappe Detlef RU; Hoppin Jane A, Measurement of novel, drinking water-associated PFAS in blood from adults and children in Wilmington, North Carolina. Environ. Health Perspect 2020, 128, 077005. [PubMed: 32697103]

(70). Hu Xindi C; Tokranov Andrea K; Liddie J; Zhang X; Grandjean P; Hart Jaime E; Laden F; Sun Q; Yeung Leo WY; Sunderland Elsie M, Tap water contributions to plasma concentrations of poly- and perfluoroalkyl substances (PFAS) in a nationwide prospective cohort of U.S. women. Environ. Health Perspect 2019, 127, 067006. [PubMed: 31170009]

(71). Liu R; Mabury SA, Synthetic phenolic antioxidants and transformation products in human sera from United States donors. Environ. Sci. Technol. Lett 2018, 5, 419–423.

(72). Chang A, Schnall AH, Law R, Bronstein AC, Marraffa JM, Spiller HA, Hays HL, Funk AR, Mercurio-Zappala M, Calello DP, Aleguas A, Borys DJ, Boehmer T, Svendsen E, Cleaning and disinfectant chemical exposures and temporal associations with COVID-19 - National Poison Data System, United States. MMWR Morb. Mortal Wkly Rep 2020, 69, 496–498. [PubMed: 32324720]

(73). US EPA, EPI Suite.

(74). Zhang X; Diamond ML; Robson M; Harrad S, Sources, emissions, and fate of polybrominated diphenyl ethers and polychlorinated biphenyls indoors in Toronto, Canada. Environ. Sci. Technol 2011, 45, 3268–3274. [PubMed: 21413794]

(75). Venier M; Audy O; Vojta š.; Be anová J; Romanak K; Melymuk L; Krátká M; Kuku ka P; Okeme J; Saini A; Diamond ML; Klánová J, Brominated flame retardants in the indoor environment — Comparative study of indoor contamination from three countries. Environ. Int 2016, 94, 150–160. [PubMed: 27248661]

(76). LeBouf RF; Virji MA; Ranpara A; Stefaniak AB, Air and surface sampling method for assessing exposures to quaternary ammonium compounds using liquid chromatography tandem mass spectrometry. Ann. Work Expo. Health 2017, 61, 724–736. [PubMed: 28927165]

(77). Stubbings WA; Schreder ED; Thomas MB; Romanak K; Venier M; Salamova A, Exposure to brominated and organophosphate ester flame retardants in U.S. childcare environments: Effect of removal of flame-retarded nap mats on indoor levels. Environ. Pollut 2018, 238, 1056–1068. [PubMed: 29703676]
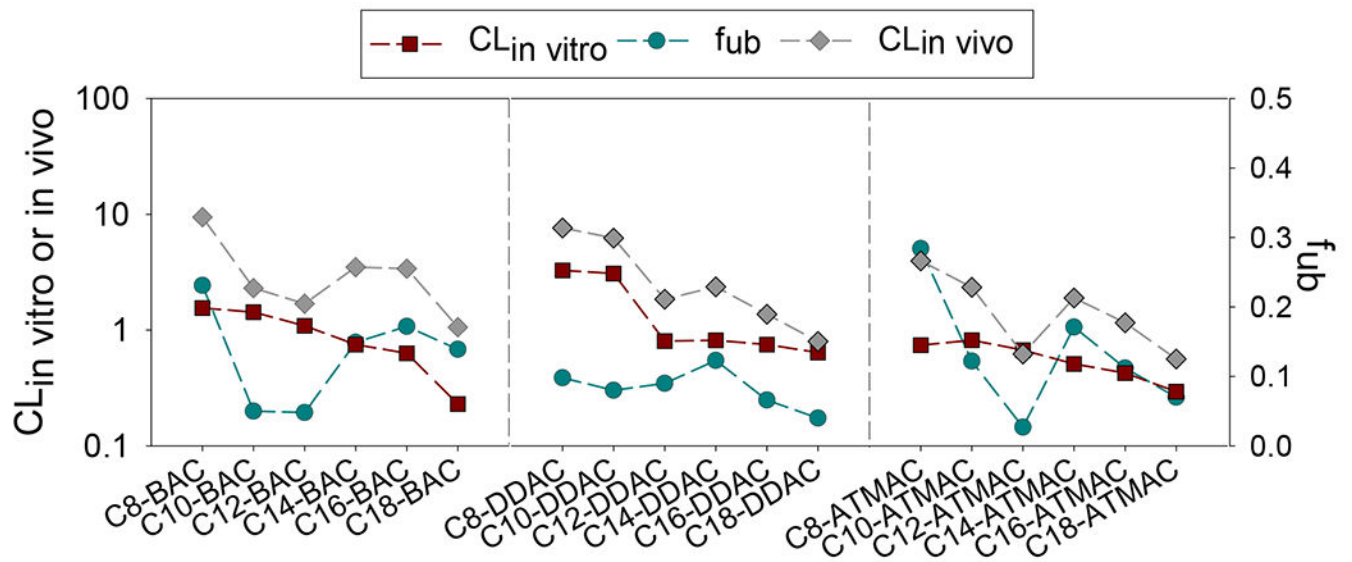
Synopsis

This study provides evidence on bioaccumulation of a wide range of QACs in human blood.
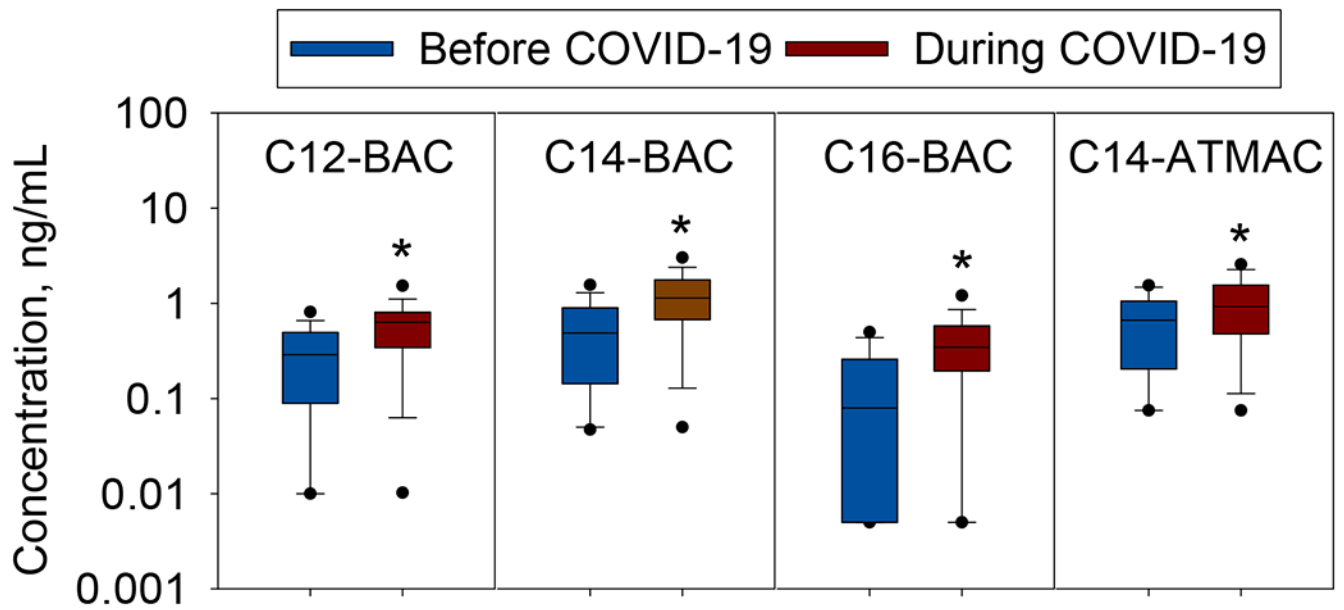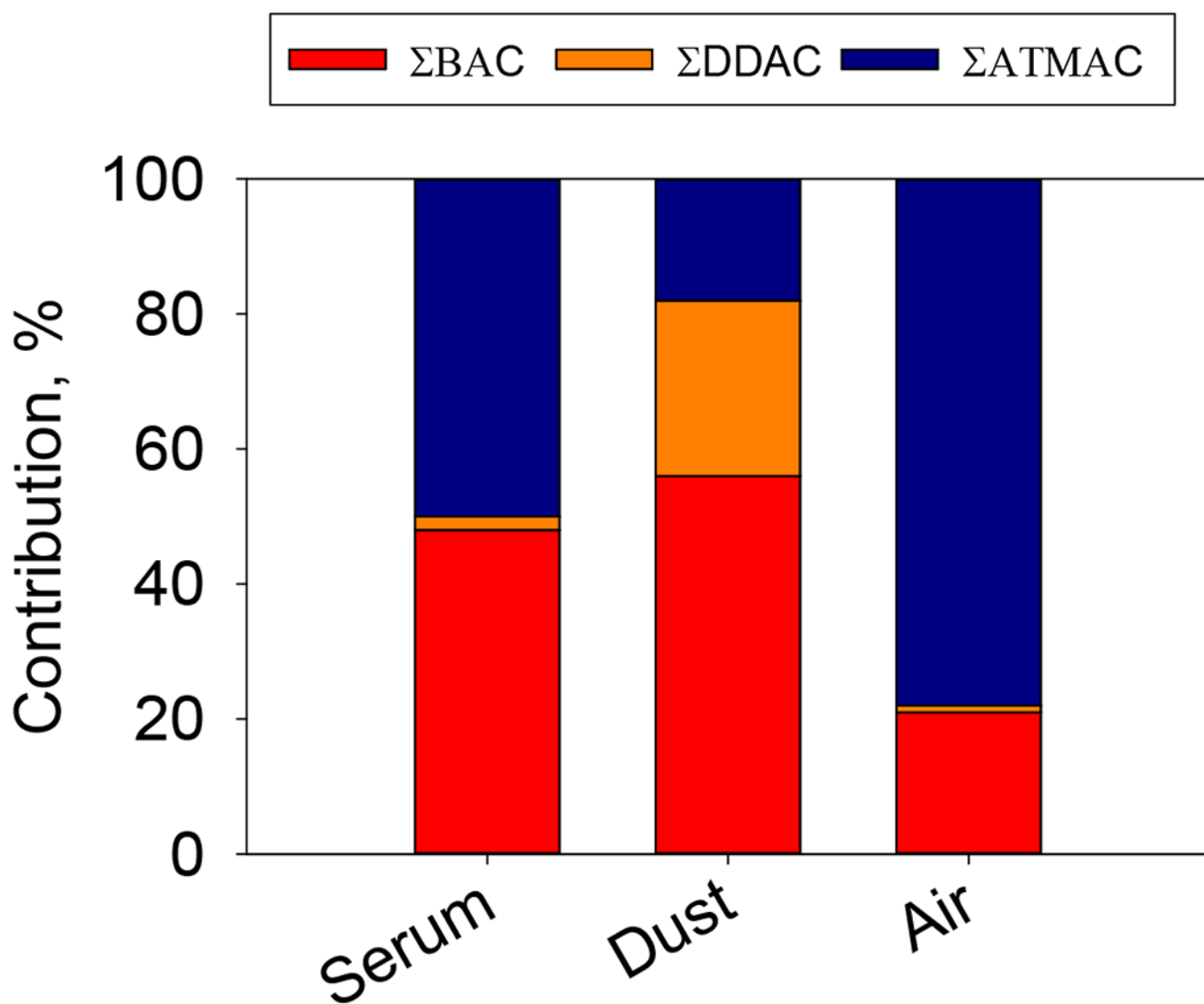
Figure 1.
The calculated *in vitro* hepatic clearance rates (CL$_{in\ vitro}$, mL/h/mg protein), unbound fractions in blood (f$_{ub}$, unitless) and *in vivo* hepatic clearance rates (CL$_{in\ vivo}$, mL/h/g liver).

Figure 2.
Serum concentrations of the select QACs detected in the samples collected before and during the COVID-19 pandemic (ng/mL). Concentrations are shown as boxplots, representing the 25th and 75th percentiles; black lines represent the median; and the whiskers represent the 10th and 90th percentiles; and the dots indicate the 5th and 95th percentiles. The asterisks represent the statistical difference at $p < 0.05$ based on a Mann-Whitney test.

Figure 3.
Comparison of the average contributions (%) of the ∑BAC, ∑DDAC, and ∑ATMAC concentrations to the ∑QAC concentrations in serum, indoor dust and indoor air collected during COVID-19. Dust data were obtained from our previous study (Zheng et al., 2020).[5] Indoor air data are based on the unpubished data[48] for the indoor passive polyurethane foam samples collected in June 2020 ($n = 6$).

Table 1.

The calculated *in vitro* hepatic clearance rates ($CL_{in\ vitro}$, mL/h/mg protein), unbound fractions in blood (f_{ub}, unitless) and *in vivo* hepatic clearance rates ($CL_{in\ vivo}$, mL/h/g liver).

QACs	$CL_{in\ vitro}$	f_{ub}	$CL_{in\ vivo}$
BACs			
C8-BAC	1.54	0.231	9.45
C10-BAC	1.43	0.050	2.31
C12-BAC	1.09	0.048	1.69
C14-BAC	0.750	0.149	3.49
C16-BAC	0.630	0.172	3.39
C18-BAC	0.230	0.139	1.06
DDACs			
C8-DDAC	1.05	0.098	3.23
C10-DDAC	0.966	0.080	2.47
C12-DDAC	0.161	0.090	0.488
C14-DDAC	0.164	0.123	0.679
C16-DDAC	0.147	0.066	0.328
C18-DDAC	0.118	0.040	0.159
ATMACs			
C8-ATMAC	0.144	0.284	1.35
C10-ATMAC	0.165	0.122	0.670
C12-ATMAC	0.127	0.027	0.114
C14-ATMAC	0.088	0.171	0.505
C16-ATMAC	0.069	0.112	0.262
C18-ATMAC	0.042	0.070	0.100

Table 2.

Detection frequencies (DF,%), minimum (min), maximum (max), and median concentrations (ng/mL) of QACs in human serum collected before ($n = 111$) and during ($n = 111$) the COVID-19 pandemic; contribution (contr, %) of each QAC to the $\sum$QAC concentrations; and percent change in concentrations measured in these two sample groups (based on median concentrations). Concentrations are calculated with the non-detects substituted with ½ method detection limit (MDL). The asterisks represent the statistical difference at $p < 0.05$ based on a Mann-Whitney test.

QACs	Before COVID-19					During COVID-19					Change, %
	DF	Min	Median	Max	Contr	DF	Min	Median	Max	Contr	
BACs											
C8-BAC	36	<MDL	<MDL	0.196	-	81	<MDL	0.055	0.433	1	-
C10-BAC	11	<MDL	<MDL	0.166	-	10	<MDL	<MDL	1.45	-	-
C12-BAC	91	<MDL	0.289	1.40	12	97	<MDL	0.634	22.1	11	120*
C14-BAC	94	<MDL	0.490	2.36	19	95	<MDL	1.14	40.1	20	132*
C16-BAC	61	<MDL	0.080	0.800	3	88	<MDL	0.346	16.4	6	334*
C18-BAC	33	<MDL	<MDL	2.14	-	72	<MDL	0.180	1.41	3	-
$\sum$**BAC**	**95**	**<MDL**	**0.893**	**5.54**	**34**	**98**	**<MDL**	**2.45**	**67.6**	**48**	**174***
DDACs											
C8-DDAC	20	<MDL	<MDL	0.447	-	5	<MDL	<MDL	0.219	-	-
C10-DDAC	15	<MDL	<MDL	0.206	-	72	<MDL	0.089	0.620	2	-
C12-DDAC	0					0					-
C14-DDAC	12	<MDL	<MDL	0.522	-	19	<MDL	<MDL	0.795	-	-
C16-DDAC	28	<MDL	<MDL	0.142	-	23	<MDL	<MDL	0.576	-	-
C18-DDAC	31	<MDL	<MDL	5.77	-	19	<MDL	<MDL	5.35	-	-
$\sum$**DDAC**	**55**	**<MDL**	**0.294**	**6.35**	**0**	**84**	**<MDL**	**0.348**	**5.76**	**2**	**18**
ATMACs											
C8-ATMAC	0					0					-
C10-ATMAC	0					0					-
C12-ATMAC	88	<MDL	0.981	8.55	39	86	<MDL	0.612	6.84	11	-38
C14-ATMAC	88	<MDL	0.667	1.86	27	94	<MDL	0.929	3.75	17	39*
C16-ATMAC	17	<MDL	<MDL	5.65	-	86	<MDL	0.966	3.53	17	-

QACs	Before COVID-19					During COVID-19					Change, %
	DF	Min	Median	Max	Contr	DF	Min	Median	Max	Contr	
C18-ATMAC	3	<MDL	<MDL	0.171	-	7	<MDL	<MDL	3.62	-	-
∑ATMAC	98	<MDL	2.03	10.2	66	97	<MDL	2.84	12.6	50	40*
∑QAC	100	0.573	3.41	13.8	100	100	0.453	6.04	68.6	100	77*